SAND2015-10505J

A highly miniaturized vacuum package for a trapped ion atomic clock

Peter D. D. Schwindt,[1,a] Yuan-Yu Jau, [1] Heather Partner, [1,b] Adrian Casias, [1] Adrian Wagner, [1] Matthew Moorman, [1] Ronald P. Manginell, [1] James R. Kellogg, [2] and John D. Prestage[2]

[1]*Sandia National Laboratories, Albuquerque, 87185, USA*

[2]*Jet Propulsion Laboratory, Pasadena, 91109, USA*

We report on the development of a highly miniaturized vacuum package for use in an atomic clock utilizing trapped ytterbium-171 ions. The vacuum package is approximately 1 cm^3 in size and contains a linear quadrupole RF Paul ion trap, miniature neutral Yb sources, and a non-evaporable getter pump. We describe the fabrication process for making the Yb sources and assembling the vacuum package. To prepare the vacuum package for ion trapping, it was evacuated, baked at a high temperature, and then back filled with a helium buffer gas. Once appropriate vacuum conditions were achieved in the package, the package was sealed with a copper pinch-off and was then pumped only by the non-evaporable getter. We demonstrated ion trapping in this vacuum package and the operation of an atomic clock, stabilizing a local oscillator to the 12.6 GHz hyperfine transition of $^{171}Yb^+$. The fractional frequency stability of the clock was measured to be $2 \times 10^{-11} / \tau^{1/2}$.

INTRODUCTION

Stable and accurate timing is critical to many modern applications ranging from navigation to communication and sensing applications. As the applications become more diverse, the size, weight, and power consumption of the timing device are critical to the feasibility of the application. Atomic clocks are the world's most accurate and long-term stable time and frequency sources, and there have been many recent efforts to miniaturize

[a] Author to whom correspondence should be addressed. Electronic mail: pschwin@sandia.gov.

[b] Current address: Humboldt University of Berlin, Newtonstrasse 15, 12489 Berlin, Germany

atomic clocks. While there has been some development in highly miniaturized laser-cooled atomic clocks,[1, 2] this development has largely been focused on vapor-cell based atomic clocks.[3-5] Vapor-cell atomic clocks typically have long-term drift due to long-term changes in the vapor cell and lamp properties.[6, 7] Buffer gas cooled trapped ion clocks, in contrast, show very little long-term instability.[8] For example, a high performance mercury ion clock has a drift rate measured to be ~10^{-17}/day.[9] Because isolation of the trapped ions from the environment is largely independent of the size of the ion trap and the surrounding vacuum package, miniaturization is readily accomplished. A lamp-pumped ^{199}Hg ion clock achieved a physics package size of ~1 L,[10] while our group developed a laser-pumped ^{171}Yb ion clock of ~0.1 L.[11] The volume of the vacuum package containing the ion trap in this clock was 3 cm^3.[12] We now report the further miniaturization of an ion trap vacuum package to a size of 1 cm^3.

There are several requirements of a miniature vacuum package for use in a trapped ion clock. It must contain the ion trap, a source of neutral Yb, and a pump to maintain appropriate vacuum conditions. The package must also have optical and electrical feedthroughs and a port to pump out the package, which can be permanently sealed in a compact way. To establish a clean vacuum environment, the package must be able to withstand a high-temperature bake of at least 250 °C, preferable 350 °C for an extended period. This precludes the use of most organic materials, such as epoxies, and typical low-temperature electronic solder alloys for either sealing the package or mounting components within the package. Additionally, the package requires a vacuum pump to maintain the appropriate vacuum environment, and it should consume no power. Finally, the package cannot contain magnetic materials since magnetic field gradients can cause motionally induced Zeeman transitions broadening the "clock" transition in $^{171}Yb^+$.[13] In the following sections, we describe a vacuum package that meets all of these requirements while occupying a volume of only 1 cm^3. Details are provided on the construction of the vacuum package, the design and implementation of the ion trap, and the fabrication of the neutral Yb sources. Finally, we show results of trapping ions in the vacuum package and the use of the ions in an atomic clock.

METAL-CERAMIC HYBRID VACUUM PACKAGE DESIGN

To meet the requirements of the vacuum package for the trapped ion clock, we chose a metal-ceramic hybrid design. Due to the size constraint of the package, the traditional glass-to-metal seal approach for electrical feedthroughs in a metal housing would take up too much space for all the required electrical connections. Contrarily, high temperature co-fired ceramic (HTCC) technology offers high density electrical feedthroughs but no simple way

to implement the optical ports in the required geometry. Our approach was to use a hybrid approach with glass-to-metal seals for the optical feedthroughs and HTCC for the electrical feedthroughs.

The metal portion of the metal-ceramic hybrid package utilized CP-2 titanium metal for the body of the package and sapphire windows to allow optical access to the trapped ions. The ceramic portion of the hybrid package allowed high density electrical feedthroughs through the use of HTCC. HTCC is a layered ceramic material system where metal traces and vias can be deposited. Electrical connections can then be established from one side of an HTCC part to the other while maintaining a hermetic seal. The HTCC forms a platform on which the ion trap is constructed and the neutral Yb sources are attached. A copper tube is attached to the package, through which the package is evacuated. This copper tube is later pinched off to permanently seal the vacuum package. For low-power operation, pumping is achieved with a non-evaporable getter, and once the getter is activated no electrical power is required to maintain the vacuum of the package. The package is assembled through a combination of high-temperature brazing and welding as described in more detail below. All of the components are non-magnetic with the exception of some nickel in the HTCC part. Nickel is used as an adhesion layer for the gold pads on the HTCC. To minimize the magnetic properties of this nickel layer, the nickel is deposited with a high phosphorous content.

The metal portion of the metal-ceramic hybrid package utilizes CP-2 titanium metal for the body of the package and sapphire windows to allow optical access to the trapped ions. The ceramic portion of the metal-ceramic hybrid package allows high density electrical feedthroughs through the use of an HTCC base. HTCC is multilayer module technology analogous to printed circuit boards where ceramic-based dielectric layers are patterned with thick film metal traces and filled vias (interlayer connections) for electrical interconnects. Thick film metal that is external to the part is plated with a metal (typically nickel and gold) compatible with solder attach, wirebonding, or potentially brazing. In this way, electrical connections can be established from one side of an HTCC part to the other while maintaining a hermetic seal through the ceramic. The HTCC then serves as a platform on which the ion trap is constructed and the neutral Yb sources are attached. A copper tube is brazed to the metal lid through which the package is evacuated. This copper tube is later pinched off to permanently seal the vacuum package. For low-power operation, pumping is achieved with a passive, non-evaporable getter, and once the getter is activated no electrical power is required to maintain the vacuum of the package. The package is assembled through a combination of high-temperature brazing and welding processes as described in more detail below. All of the components are non-magnetic except the plated HTCC nickel. Nickel is used as a solderable metallization which is

passivated from oxidation by plated gold on the HTCC externally exposed traces. To minimize the magnetic properties of this nickel layer, the nickel is deposited with moderate phosphorous content.

The hybrid metal-ceramic vacuum package is a complex part involving the procurement of many custom components and multiple specialized assembly steps. In the construction of the hybrid vacuum package, two primary components are fabricated (Figure 1). The first is the vacuum package lid that is made using metal vacuum packaging techniques, and it incorporates sapphire viewports and the copper tube through which the vacuum package is evacuated. The second component is the ion trap assembly that is made using ceramic packaging techniques, and it is built up on an HTCC part. The lid and the ion trap assembly are brought together in a final welding step to complete the fabrication of the package. After fabrication, the vacuum package is attached to a vacuum system to establish a good vacuum environment and to test the operation of the ion trap prior to the final pinch-off of the copper tube.

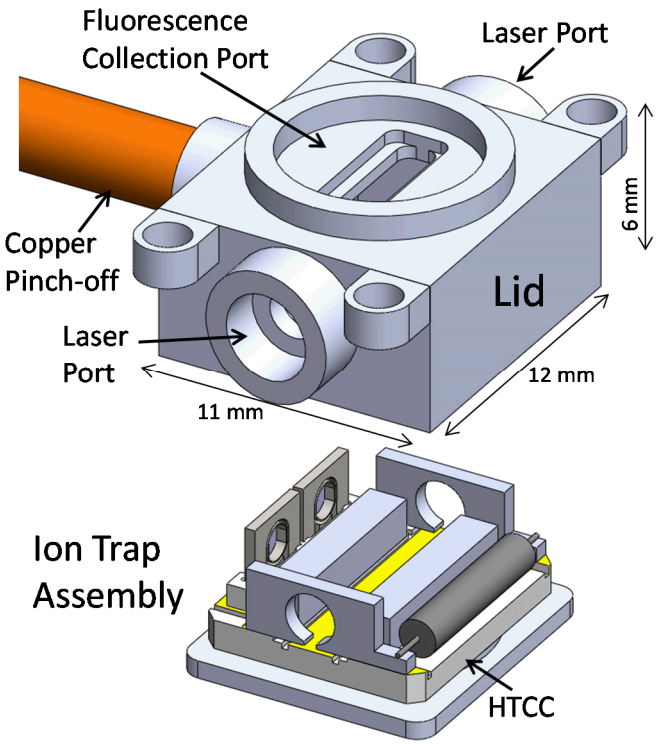

Figure 1. Solid model of the metal-ceramic hybrid package with the ion trap assembly and the lid separated so that the components of the ion trap assembly are visible.

The lid was custom built to our design by IPT-Albrecht, GmbH (Schwanau, Germany). The body is made of a machined CP-2 titanium shell. Sapphire windows are brazed into titanium sleeves and then laser welded into the lid body. Sapphire has a coefficient of thermal expansion that is reasonably well matched to titanium, critical for a sapphire to titanium hermetic braze interface. The laser ports are made up of two 3-mm diameter windows to allow laser light to pass along the length of the ion trap. There is a 2-mm aperture machined into the titanium body just inside each 3-mm window, and the 3-mm windows are mounted at a 6° angle to prevent light reflecting back to the laser sources. On the top of the lid, there is a fluorescence collection port comprised of a 6.5-mm diameter window with a 1.5 mm × 6 mm aperture. This window allows the collection of fluorescence from the trapped ions. After the sapphire windows have been brazed into their titanium sleeves but prior to welding the windows to the lid, they are anti-reflection coated to minimize reflections at 297 nm, 369 nm and 935 nm. A 30-mm long, 3-mm inner diameter copper tube is brazed into one wall of the lid prior to welding of the viewports. At the other end of the copper tube, a 1.33 inch ConFlat® flange is brazed to allow attachment to a vacuum system.

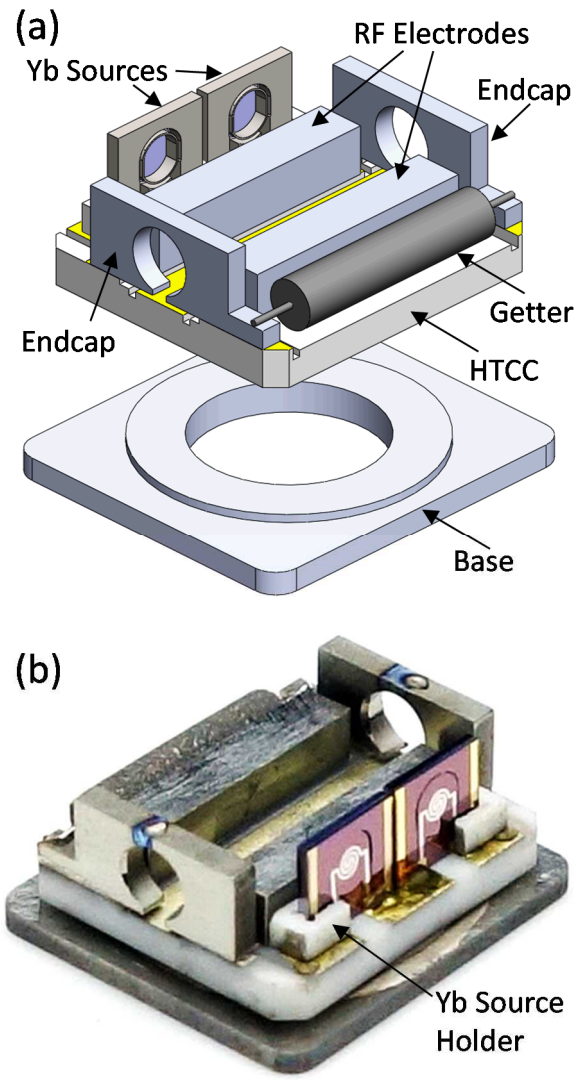

Figure 2. (a) Three dimensional illustration of the ion trap assembly where the titanium base is separated from the HTCC to show the raised ring to which the HTCC is brazed. (b) Photograph of the completed ion trap assembly (opposite side view from 'a').

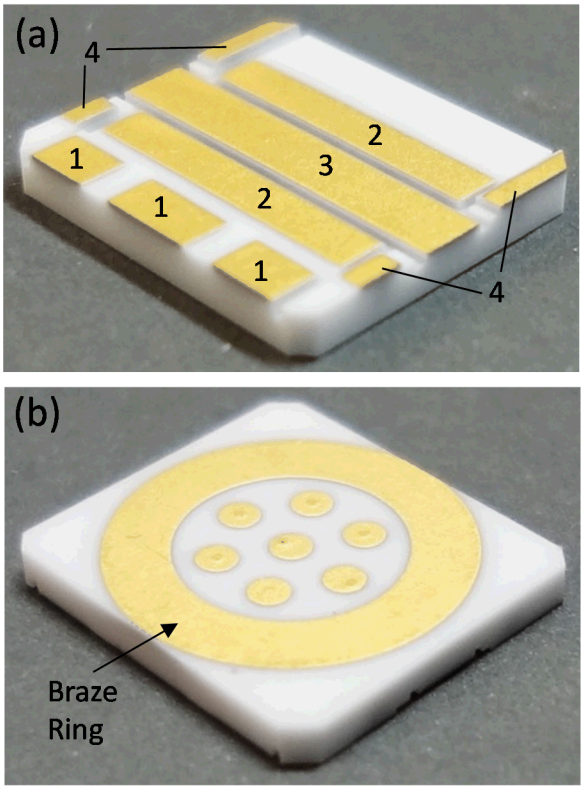

Figure 3. (a) Photograph of the top side of the HTCC part. The gold pads are for the following: 1. Solder pads for the Yb sources. 2. Braze pads for the RF electrodes. 3. RF ground electrode. 4. Braze pads for the endcap electrodes. (b) Photograph of the bottom side of the HTCC part. The seven small circular pads provide external electrical connections for the internal surface mount pads inside the vacuum package. The gold ring surrounding the external electrical connections is where the braze interface between the HTCC part the titanium base is formed. The dimensions of the HTCC part are 9.8 mm × 8.8 mm × 1.15 mm.

The ion trap assembly (Figure 2**Error! Reference source not found.**(b)) contains all of the electrically active components of the vacuum package except the top electrode. The active components are assembled on the surface mount pads on the "top" of the HTCC part (Figure 3(a)). These pads are electrically connected through the HTCC part by metal thick film traces and vias passing through the HTCC dielectric to small circular pads on the "bottom" of the HTCC part (Figure 3(b)). There are several trenches between the gold pads on the top of the HTCC part to prevent shorting of the electrodes when Yb is deposited during the trap loading process. The ring on the bottom of the HTCC part is where the titanium base is brazed to the HTCC. The base and the trap electrodes are made from CP-2 titanium and are attached to the HTCC with a copper (28% by mass) silver (72% by mass) braze

alloy (trade name of Cusil) in a single step process. The Cusil alloy has a liquidus at 780 °C, and the braze furnace peak process temperature was 810 °C to ensure complete melting. After brazing, the braze joint between the HTCC and the Ti base was checked for hermeticity by a He leak test. The braze process produced a leak-free ($< 10^{-10}$ atm*cc/s He) HTCC-titanium interface for roughly half of the part fabricated. Cracking in the HTCC would frequently be observed although the cracks did not necessarily cause a leak. These problems were attributed to stress developing when the assembly was cooled down to room temperature. While the coefficient of thermal expansion (CTE) of Ti (~10.1 ppm/°C) and HTCC (~7.4 ppm/°C) are fairly well matched, finite element modeling indicated that the relatively large thickness of the Ti components caused significant stress in the thinner HTCC part as it was cooled down. This stress was further enhanced by location of the trenches in the HTCC with respect to the Ti components. A redesign of the trench geometry and thickening of the HTCC part to redistribute and reduce the stress on the HTCC would likely significantly improve the reliability of the braze process. Also, other metals with a better CTE match to HTCC could potentially be found to reduce stress in the HTCC.

If the Ti-HTCC braze joint had no detectable leak, the miniature Yb sources and the getters were attached. The Yb sources are attached with a gold (87.5% by mass)-germanium (12.5% by mass) solder (trade name of Georo). Au-Ge solder has a liquidus of 361 °C, and is one of the higher melting point solders that does not contain zinc. A process temperature of 405 °C ensures reflow of the Georo solder. The solder process is done in an Ar atmosphere to mitigate Yb evaporation, which in a vacuum process was significant. The Ar atmosphere also helped with more uniform heating of the assembly during the solder process. A higher temperature compatible solder was desired, but not located due to a lack of vacuum compatible solders between the high temperature solder and low temperature braze alloys. Essentially, as high of a melting point as possible is desired to maximize the temperature of the bake-out process when the package is being evacuated in preparation for ion trapping and eventual copper tube pinch-off. However, the temperature of the bake-out is ultimately limited by the evaporation of the Yb which must be minimized during bake-out. The final step in making the ion trap assembly is spot welding the getter to the endcap electrodes. The getter is formed from the ST-172 alloy from SAES, chosen for its relatively low activation temperature. It is 1.5 mm in diameter and 7 mm long and has a tungsten wire passing through its long axis. The spot welding process seems to mainly melt the Ti and not the tungsten wire, but the Ti captures the tungsten wire forming a good mechanical and electrical connection.

The final step in the assembly process of the vacuum package is the welding of the base to the lid. Before the final weld, both base and lid subassemblies were carefully and somewhat blindly aligned, clamped together, and then all electrical networks were verified for continuity and discontinuity. We used an electron-beam weld process in a vacuum environment. The success of the weld depends critically on the parameters of the weld process, tight tolerance of the mating surfaces, and cleanliness in the weld vicinity. With too little energy in the e-beam, the weld would not seal the package, and with too much energy, the base would stress to the point where the HTCC part would crack, causing a leak. As seen in Figure 4, the *e*-beam weld seam goes around the perimeter of the base, and the kerf of the weld is ~0.5 mm. To limit the temperature rise of the package during the welding, the *e*-beam is pulsed and laterally stepped before pulsing again. Continuous welding, in contrast, would cause much greater temperature increases than pulsed welding. We found the pulsed technique to form a very reliable weld with no failures in the six builds of the package.

Figure 4. Photograph of the completed hybrid metal-ceramic vacuum package. Note the e-beam weld seam.

ION TRAP DESIGN

To confine the ions in the vacuum package, we used an RF Paul trap in a linear quadrupole configuration. Because of the small size of the vacuum package, the walls of the vacuum package need to be carefully considered in the design of the ion trap. In fact, to maximize the degree of package miniaturization, the walls are used as electrodes in the ion trap. This leads to a geometry that is modified compared to a more typical four-rod quadrupole trap. Figure 5(a) shows the geometry of the trap electrodes used in modeling the ion trap. The endcap electrodes are shown in blue in Figure 5(a). Their geometry in the model is substantially different from the geometry of the Ti endcaps actually used in the trap as seen in Figure 2(a), but this difference in geometry has almost no influence since

the endcap potential has little (less than 1%) effect on the trapping potential, particularly near the center of the trap. The RF electrodes (green in Figure 5) are formed by the Ti bars brazed to the HTCC as seen in Figure 2(a). The lower RF ground electrode (dark red in Figure 5) is formed by the central gold pad on the HTCC part (pad 3 in Figure 3(a)), and the upper RF ground electrode is split in half and is formed by the Ti lid (Figure 1). Fluorescence from the ions is collected through the gap in the upper RF ground electrode.

To determine if this nonstandard electrode geometry would trap ions, we numerically modeled the electric fields of the ion trap and evaluated its total potential. In the RF Paul trap, the electric potential on the RF electrodes is rapidly varied and the time average of the RF electric fields generated between the electrodes can be evaluated to give the pseudopotential $\Psi(x,y,z) = \frac{q}{4m\Omega^2} E_{RF}^2(x,y,z)$, where q is the charge of the ion, m is the mass of the ion, $\Omega/2\pi$ is the frequency of the RF, and $E_{RF}(x,y,z)$ is the electric field due to the applied RF potential.[14, 15] The total trap potential is then found by summing the RF pseudopotential with the potential due to the DC voltage applied to the endcaps. The total potential in the transverse plane is shown in Figure 5(b) and at this location is largely due to the RF pseudopotential. The gap in the upper RF ground electrode gives rise to a low point in the trap potential through which the ions can escape. The width of this gap must balance the need for a deep trapping pseudopotential, which requires narrower gaps, and the need for maximal fluorescence collection, which requires wider gaps. We chose a 1.5 mm width for the gap giving a ~15° angle for fluorescence collection and a trap depth of 1.0 eV for the actual experimental voltages used (RF frequency 2.88 MHz, amplitude 155 V), sufficient for trapping buffer gas cooled ions. In addition to the pseudopotential, we evaluated the stability of the ion trap with respect to the micromotion induced by the oscillating electric fields, following the formalism developed in Reference 16, and the model indicated stability in the trapping region.

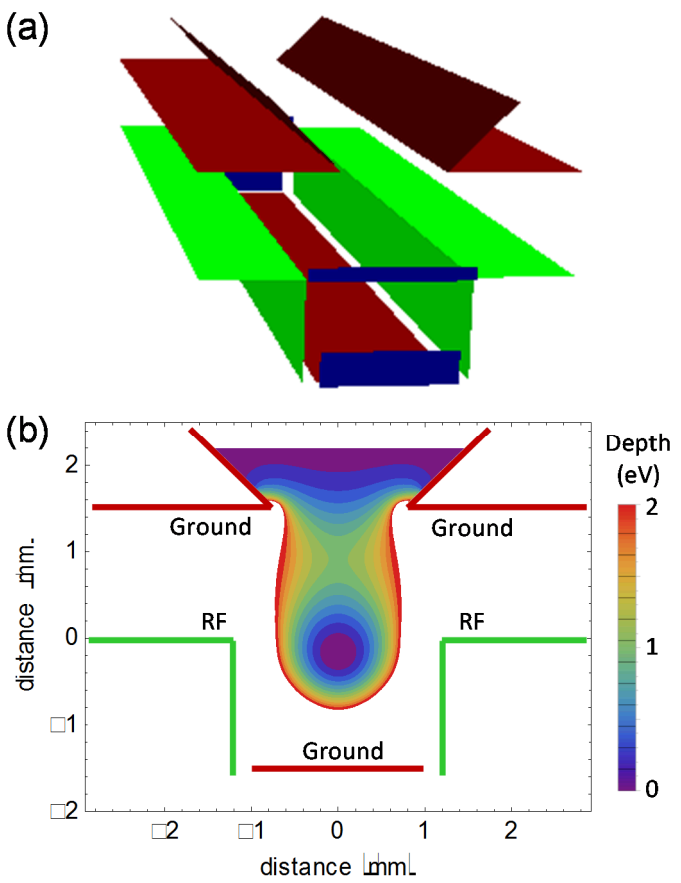

Figure 5. (a) Image showing the electrodes used in the model of the ion trap. The green electrodes are the RF electrodes. The dark red electrodes are the RF ground electrodes. The upper two RF ground electrodes are formed by the titanium lid and the lower RF ground electrode is gold pad on the HTCC part. The blue electrodes are the endcaps. (b) Contour plot of the transverse pseudopotential of the ion trap showing the depth of the trap to be 1.0 eV.

MINIATURE Yb SOURCE DEVELOPMENT

One of the principal components of the miniature vacuum package is the Yb source. The package requires a source that has a very small size and does not require a great deal of power to produce Yb vapor in the center of the ion trap. We chose a microfabricated silicon "hotplate" as a platform for the Yb source. A previous version of the miniature hotplate was described in Reference 17, and here we describe improvements in the Si hotplate and a new high-efficiency filling technique using evaporation of Yb.

A. Si hotplate fabrication

The Si hotplate structures are built from silicon-on-insulator (SOI) wafers. Deep-reactive-ion etching (DRIE) is used to etch through both the 400-μm-thick handle wafer and the 20-μm-thick top layer of the wafer (also called the device layer). Each layer is etched with a different photo-lithographically defined pattern to create a three-dimensional cup structure on the backside of the SOI handle layer into which the Yb will be deposited (Figure 6). The Yb-holding cup is suspended by narrow beams formed in just the device layer (Figure 6(a)) or in both the device and handle layer (Figure 6(b)). These narrow beams limit the thermal conduction from the cup to exterior sections of the Si hotplate structure. In the previous version of the hotplates,[17] the device layer was a highly-doped (low-resistivity) silicon. To heat the hotplate, current was passed through the device layer. However, most of the heat was deposited in the narrow beams supporting the Yb cup and not in the cup itself. To alleviate this problem, we switched to a high-resistivity silicon in the device layer, and we now deposit a platinum heater element on the Si hotplate to generate heat primarily in the center of the Yb-holding cup. The 200-to-300-nm-thick Pt film of the heater element is deposited on a 20 nm ZnO adhesion layer (Figure 6(d)). The ZnO film is critical because it not only serves to adhere the Pt to the Si, but it minimizes both the diffusion of the Pt into the underlying Si substrate and the free energy of the Pt thin film, which limits the agglomeration of the metal at elevated temperatures.[18] The ZnO layer allows us to operate the Pt heater lines at significantly elevated temperatures and for longer time periods compared to traditional Ta or Ti adhesion layers.

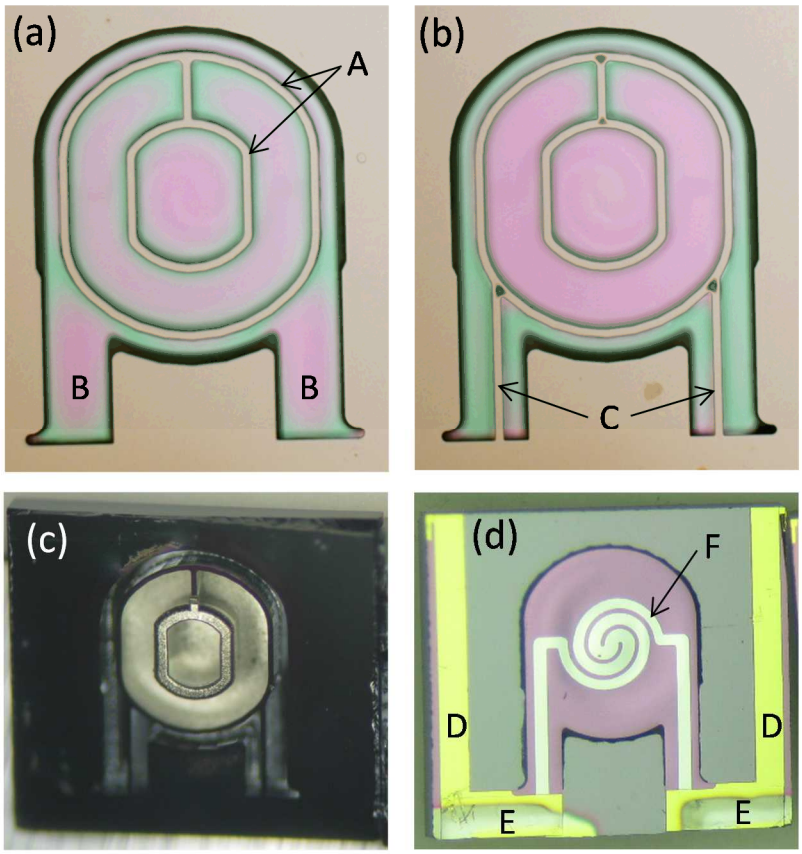

Figure 6. (a) Photo of the cup structure of the Si hotplate. A. The full-wafer-thickness structures that define the cup that holds the Yb. B. The narrow beams that support the suspended Yb-holding cup. (b) Photo of another design for the Si hotplate where a full-wafer-thickness stiffener is added to strengthen the support beams as indicated by C. (c) Photo of a Si hotplate that has been filled with Yb. Note how the Yb is deposited both down at the bottom of the cup and on the top of the inner ring of the support structure. (d) Photo of the device layer side of the Si hotplate. D. The L-shaped Cr/Au pads that are on the top of the wafer only. E. The Ti/Pt/Au edge metallization is wrapped over the top of the Si hotplate to allow subsequent edge mounting as discussed in the text. F. The Pt heater element.

A shown in Figure 2(b), the Si hotplates are mounted to the HTCC part on their lower edge. The trap design necessitates this so that Yb vapor is directed toward the center of the ion trap. However, forming a robust mechanical and electrical connection in this edge-mount configuration is challenging. This is accomplished in the following way. Lithographically-defined, L-shaped, 20 nm Cr/ 750 nm Au pads are deposited on the top of the device layer, which overlap the Pt heater element and extend to the lower edge of the Si hotplate (D in Figure 6(d)).

In the construction of the wafer, the wafer is etched completely through, exposing the lower edge of the Si hotplates. An alumina shadow mask is then placed over the wafer which allows metal to be sputtered to cover both the Cr-Au pads and the bottom edge of the hotplate device (Figure 7). This metallization is composed of 500 nm Ti/ 1000 nm Pt/ 1000 nm Au as measured on a flat, normal surface. The wafer was mounted at a 30° angle inside the sputter chamber to allow some line of sight to the exposed edges of the Si hotplates. Thus, the edge metallization was some undetermined amount thinner than if it were deposited on a flat surface. After metallization, a dicer singulated the wafer to form individual 3 mm × 3 mm devices. After the Si hotplate cup is filled with Yb, the miniature Yb source is soldered to the HTCC parts using the edge pads and the Au-Ge solder. To limit the deposition of Yb onto the HTCC part once the Yb source is operational in the vacuum package, a laser-cut alumina fixture (called the Yb source solder in Figure 2(a)) surrounds the base of the Yb sources. The fixture is also metallized with sputtered Ti/Pt/Au both on its bottom and interior edges in the places where the fixture overlaps the gold pads on the HTCC and the Yb sources. In addition to preventing shorting between components mounted on the HTCC part, the Yb source holder provides additional mechanical strength to the edge mount solder connection.

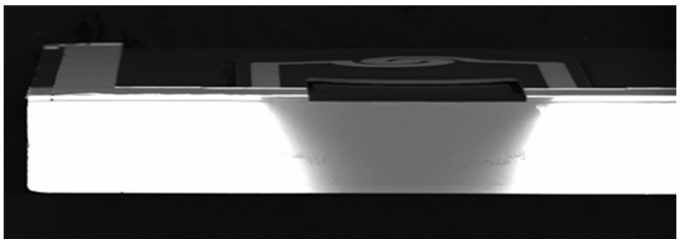

Figure 7. SEM image of the edge of the Si hotplate after sputtering of the edge metallization. The bright white areas are where the metal is deposited.

B. Loading the Yb sources

In Reference [17], we described two filling techniques to deposit Yb in the cup of the Si hotplate: a liquid ammonia dissolution technique and a standard evaporation technique using an *e*-beam evaporator. The primary problem with the evaporation technique was that it is a very inefficient use of Yb. The ion trap is best loaded from an isotopically enriched ^{171}Yb source since the primary technique for ionizing the Yb is not isotopically selective.[12] However, isotopically enriched ^{171}Yb is very expensive and not appropriate for standard *e*-beam evaporation. The liquid ammonia dissolution of the Yb directly in the cup of the hotplate and subsequent precipitation is highly

efficient and deposits a large fraction of the Yb in the cup. However, the Yb would often splash over the edges of the hotplate cup. In addition, the Yb in the cup would be very porous, having a great deal of surface area. This would cause there to be a large amount of oxidized ytterbium after the Yb was exposed to air, reducing the amount of Yb metal available for re-evaporation. We now have developed a miniature evaporation technique that efficiently deposits the Yb in the cup of the Si hotplate, with a minimum of exposed surface area.

To transfer a small amount of Yb into the Si hotplate, the Yb and the Si hotplate are assembled into a miniature evaporation fixture (Figure 8). On a 0.6-mm-thick Si wafer, a piece of Yb metal, typically 1 to 2 mg, is placed. Over the Yb metal piece, a 1.47-mm-thick glass rectangle with a tapered hole is placed. The hole is ultrasonically machined into the glass with the bottom of the hole being 1.5 mm in diameter and the top being 0.7 mm in diameter. The glass rectangle and the Si hotplate are aligned to each other using four layers of laser cut alumina fixtures, all 0.5 mm thick. The alumina layers are aligned to each other using two alumina rods 0.75 mm in diameter. The layers 1 and 2 hold the glass rectangle. Layer 3 supports the Si hotplate over the glass and the 1-mm-diameter hole in this layer provides a shadow mask. Layer 4 aligns the Si hotplate to the holes below it.

The evaporation assembly is then transferred to a vacuum chamber and placed on a boralectric heater. The chamber is evacuated to a pressure of 10^{-7} to 10^{-6} Torr. A constant voltage is applied to the boralectric heater so that in 4 minutes the temperature of the boralectric heater reaches ~600 °C. The boralectric heater is maintained at a temperature of 615 °C to 620 °C for two hours. Typically 30 to 50% of the Yb is transferred into the Si hotplate cup, resulting in 0.5-0.8 mg of Yb being deposited. A photograph of a filled Yb source is shown in Figure 6(c). We tested evaporation of the Yb at ~800 °C. While the Yb could be transferred in 3 to 4 minutes at this temperature, the gold metallization on the edge of the part would disappear, rendering the part useless since the Ge-Au solder would no longer flow onto the edge metallization in subsequent assembly steps. At these elevated evaporation temperatures, we believe increased heat transfer to the silicon chip caused the gold on the lower edge of the Si hotplate to diffuse into the Si. Energy dispersive x-ray spectroscopy of such surfaces showed a reduction of edge gold relative to samples treated at lower temperatures. Another difficulty in the evaporation of the Yb is the large difference in the coefficient of the thermal expansion between Yb (26.3×10^{-6} K^{-1}) and Si (2.6×10^{-6} K^{-1}). At its thickest near the center of the cup, the deposited Yb is estimated to be 15 to 30 μm thick. Cracking of the Si device layer can occur both when the device is first cooled down after Yb deposition into Si hotplate and then later in the repeated heating and cooling cycles while the Yb source is in use. This cracking problem is largely alleviated by the interior full-

wafer-thickness ring in the hotplate cup, which provides sufficient support to the 20-µm-thick device layer. Previous Yb sources with only the exterior ring would frequently crack.

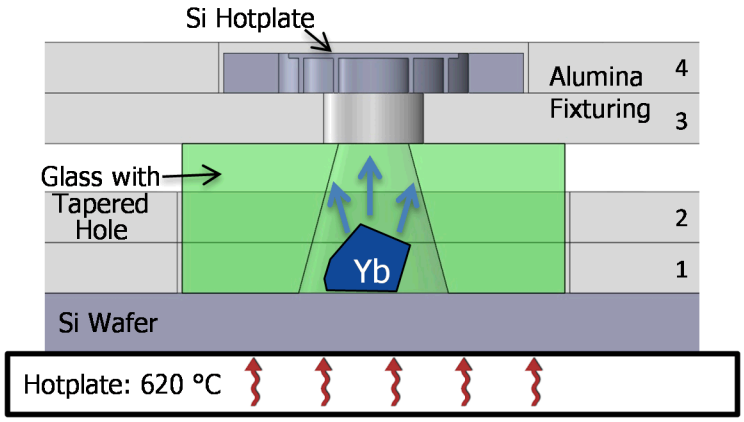

Figure 8. Cross-section of a schematic of the miniature evaporation fixture for depositing Yb into the Si hotplate. The numbers label the layers of alumina fixturing.

RESULTS

Once the assembly of a vacuum package was completed, it was attached a vacuum system to prepare the appropriate vacuum conditions inside the package. The vacuum package was heated to 250 °C for 2.5 days. This bake-out process not only desorbs residual gases from the walls and components of the vacuum package but also serves to partially activate the non-evaporable getter. While the vacuum package is designed to be baked up to 350 °C, we chose the more conservative temperature to reduce the chances of cracking the ceramic and sapphire components and causing a leak. Future vacuum packages will be baked at a higher temperature to improve the vacuum conditions and provide better activation of the getter. At the completion of the bake-out it was verified that the getter was pumping nitrogen as observed on the residual gas analyzer attached to the vacuum system. The final vacuum preparation is to introduce a helium buffer gas to the system at a pressure of 2×10^{-6} Torr. The helium serves as a cooling mechanism for the ions in the trap since the RF Paul trap tends to heat the ions out of the trap. Although not directly measured in this ion trap, the ion temperature at this helium pressure was measured to be ~1000 K in a previous vacuum package.[12]

With the vacuum conditions prepared in the vacuum package, we verified Yb source operation and ion trapping prior to the final copper pinch-off sealing of the vacuum package. This is particularly important since when

the Yb sources are first activated, they release a significant amount of gas that is best pumped away by the large vacuum system and not by the internal getter. To verify Yb vapor production, we passed a 399 nm laser, resonant with the $^1S_0$ to $^1P_1$ transition in neutral Yb, through the center of the ion trap and observed the fluorescence on a camera. Of the ovens mounted in the vacuum package, one was loaded with Yb of natural abundance and had the Si hotplate design of Figure 6(b) with the full-wafer-thickness support beams, and the other was loaded with isotopically purified ^{171}Yb and had the design of Figure 6(a) with support beams being made from only the device layer. From previous experiments, we know that neutral fluorescence is observed at 420 to 450 °C. For the natural abundance Yb source we observed fluorescence with a voltage and current on the heater element of 3.3 V and 320 mA while the ^{171}Yb oven required 1.5 V and 170 mA. The natural abundance Yb source required four times more power because the thicker support beams increased the thermal losses from the hotplate cup. We chose to include the higher power design because it is much more mechanically robust. To ionize the neutral Yb in the trap region, we used two-photon photoionization, where the absorption of a 399 nm photon and a 369 nm photon will ionize the atom. The voltages to the ion trap were 310 V_{PP} at a 2.88 MHz applied to the RF electrodes and 20 V applied to the endcap electrodes. We found that voltages between 5 and 20 V on the endcaps would work nearly equally as well with a slight preference toward 20 V. We estimated that roughly 10^4 ^{171}Yb ions were loaded in the ion trap under these conditions. With all of the functions of the vacuum package verified, we proceeded to seal the cell by pinching off the copper tube forming a cold weld seal. The final hybrid vacuum package is ~1 cm^3 in size and requires no active vacuum pump (Figure 9).

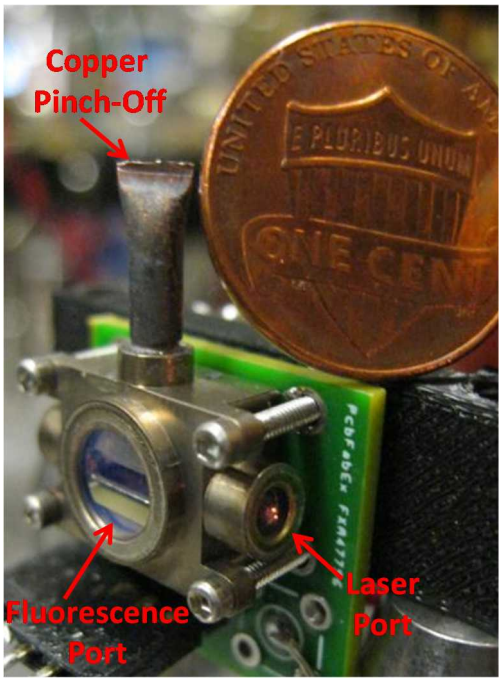

Figure 9. Photo of the pinched-off hybrid metal-ceramic vacuum package.

The vacuum package was operated as part of an atomic clock in a table-top clock system. In this system the ^{171}Yb ions were first prepared in the $^2S_{1/2}$, $F = 0$ hyperfine ground state. The 12.6 GHz microwaves were then applied to the ^{171}Yb ions to drive the hyperfine transition to the $^2S_{1/2}$, $F = 1$ hyperfine state. Next, the number of ions that underwent the transition to the $F = 1$ state was detected by applying the lasers at 369 nm to drive the $^2S_{1/2}$ to $^2P_{1/2}$ transition and at 935 nm to drive the $^2D_{3/2}$ to $^2\mathrm{D}[3/2]_{1/2}$ transition. Fluorescence from the $^2\mathrm{D}[3/2]_{1/2}$ to the $^2S_{1/2}$ transition was collected to determine the number of ions that were in the $F = 1$ ground state. The state detection lasers also served to optically pump the ion back to the $^2S_{1/2}$ $F = 0$ ground state so the clock cycle could begin anew. An error signal was derived from the fluorescence signal that was subsequently used to correct the frequency of the local oscillator that provides the 12.6 GHz microwaves. The microwave interrogation time was 700 ms (-54 dBm from our synthesizer was required for the π-pulse) and the state detection/optical pumping time was 300 ms with 17 μW of light at 369 nm and 2.9 mW at 935 nm. The fluorescence signal was collected with a photomultiplier tube for the first 100 ms of the state detection/optical pumping pulse. The power of the 399 nm laser was 2.9 μW for the two-photon photoionization. Under these conditions the clock demonstrated a fractional frequency instability of $2\times10^{-11}/\tau^{1/2}$, where τ is the averaging time of the measurement (Figure 10). It is important to note that the clock algorithm used to lock the LO to the ions had a technical problem where the computer controlling the frequency of the LO was

not well synchronized with the clock cycle and thus every other clock cycle measurement was discarded increasing the dead time in the clock loop from 300 ms to 1300 ms. If this dead time were eliminated, we estimate a stability of $1.4\times10^{-11}/\tau^{1/2}$.

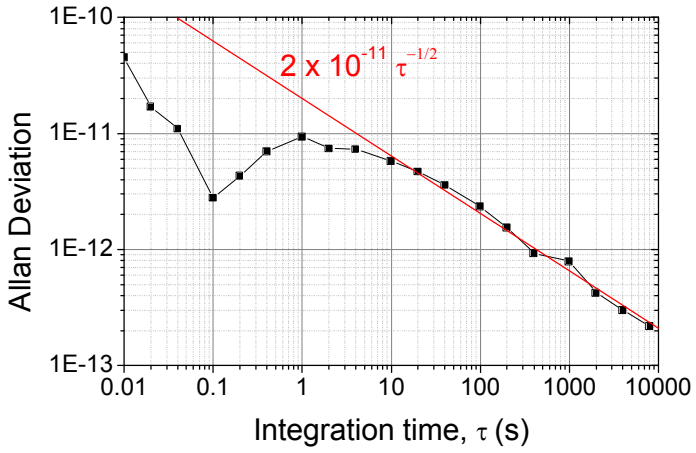

Figure 10. Performance of the hybrid metal-ceramic vacuum package in an atomic clock.

We also measured the coherence time of the clock transition (Figure 11). This was done by first preparing the ions in the $F = 0$ state, applying a varied microwave pulse length, and then measuring the fluorescence indicating the population of the $F = 1$ state. Fitting this data gave a T_2 of 19 ± 4 s, showing the exceptionally long coherence time of the trapped ions. We suspect that this is limited by a combination of gradients in the magnetic field across the ion trap and temporal magnetic field instability since no magnetic shields were used for the measurement. A final measurement of the quality of the vacuum package is the lifetime the ions in the ion trap. This was measured to be approximately 50 hours, eight days after the vacuum package was pinched-off.

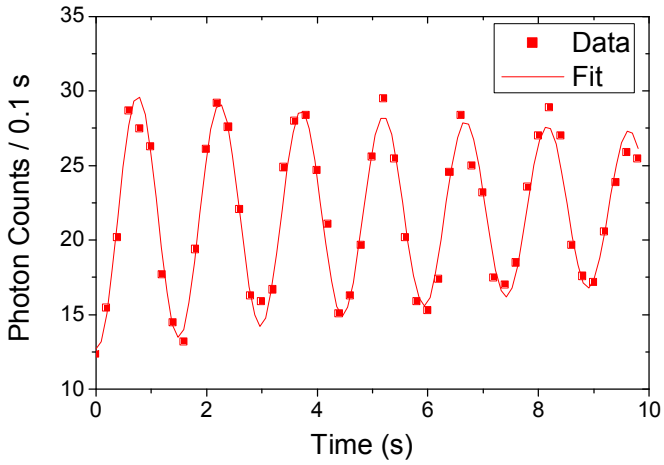

Figure 11. A measurement of the coherence time of the trapped ion. The photon counts for a 0.1 s gate time are plotted against the microwave interrogation time. Each data point is an average of 16 measurements.

CONCLUSION

These results demonstrate several important aspects of the creation of an ultra-miniature atomic clock package. The hybrid metal-ceramic vacuum package technology is clearly viable for use in a Yb ion clock. The clock performance of this 1 cm^3 package is nearly identical to that achieved in our previous 3 cm^3 package showing that the miniaturization of the package while maintaining a similar ion trap size does not degrade the clock operation. We developed an improved miniature Yb source and have demonstrated for the first time the use of a microfabricated Yb source in a miniature vacuum package. An open question for the vacuum package is whether or not these packages can support a much longer trapped ion lifetime, necessary for clock operation over several years. The lifetime in the hybrid package is about an order of magnitude shorter than previous vacuum packages we have built.[12] It is likely that a hotter and longer bake-out in the preparation of the vacuum package will drastically improve the trapped ion lifetime. The hybrid package should be able to sustain baking to 350 °C. The primary limits are the melting point of Ge-Au solder (361 °C) used for attaching the Yb sources and the evaporation and migration of the Yb metal. Usually an oxide crust on the Yb metal will keep the Yb in place until the crust is broken through in the first activation of the oven, but it may be the case that an extended bake near 350 °C may allow Yb to migrate around the package causing shorting of the trap electrodes. Typically as vacuum conditions and the lifetime of the trapped ions improve, the ions can be trapped in the long-lived low-lying $^2F_{7/2}$ state of Yb during clock operation, reducing the number of ions participating in the clock measurement. We did not observe *F*-state trapping the hybrid

package, but if this occurs in improved packages in the future, a small amount of methane buffer gas could be added to alleviate the *F*-state trapping.[19]

While this package was developed for an atomic clock, the hybrid metal-ceramic vacuum package with microfabricated Yb sources could find use in other trapped ion applications, particularly trapped ion quantum computing. Ion traps for quantum computation are becoming increasingly complex with numerous electrodes.[20] There is also a need to miniaturize the vacuum chambers for the ion traps if trapped ion quantum computing is to become scalable. HTCC can readily allow a large number of electrical feedthroughs while also forming a hermetic air-vacuum interface. The Yb source would also be an ideal source for neutral Yb in a miniaturized quantum computing vacuum package. Overall, we have developed a new miniaturized vacuum package for trapped ion atomic clocks with potential use in other applications, and continued development will lead to its use in truly practical devices.

ACKNOWLEDGEMENTS

The authors thank John Anderson for aid in the fabrication of the silicon hotplates and Jeff Hunker for experimental support. Sandia National Laboratories is a multi-program laboratory managed and operated by Sandia Corporation, a wholly owned subsidiary of Lockheed Martin Corporation, for the U.S. Department of Energy's National Nuclear Security Administration under contract DE-AC04-94AL85000. This research was developed with funding from the Defense Advanced Research Projects Agency (DARPA). The views, opinions, and/or findings contained in this article are those of the authors and should not be interpreted as representing the official views or policies of the Department of Defense or the U.S. Government. Approved for public release, distribution unlimited.

REFERENCES

[1]K. Salit, J. Sebby-Strabley, K. Nelson and J. Kriz, *Progress on the Cold Atom Micro Primary Standard (CAMPS)*, *Proceedings of the IEEE International Frequency Control Symposium* Baltimore, MD, USA, 21-24 May 2012, pp. 1-4.

[2]V. Shah, R. Lutwak, R. Stoner and M. Mescher, *A compact and low-power cold atom clock*, *Proceedings of the IEEE International Frequency Control Symposium (FCS)*, Baltimore, MD, USA, 21-24 May 2012, pp. 1-6.

[3]S. Knappe*, et al.*, Appl Phys Lett **85**, 1460-1462 (2004).

[4]R. Lutwak*, et al.*, *The miniature atomic clock - Pre-production results*, *Proceedings of the IEEE International Frequency Control Symposium-Jointly with the European Frequency and Time Forum*, Geneva, Switzerland, 29 May-1 June 2007, pp. 1327-1333.

[5]L. Maleki*, et al.*, *All-Optical Integrated rubidium Atomic Clock*, *Proceedings of the Joint Conference of the IEEE International Frequency Control and the European Frequency and Time Forum* San Fransisco, CA, USA, 2-5 May 2011, pp. 1-5.

[6]J. C. Camparo, C. M. Klimcak and S. J. Herbulock, IEEE Trans. Instrum. Meas. **54**, 1873-1880 (2005).

[7]S. Abdullah, C. Affolderbach, F. Gruet and G. Mileti, Appl Phys Lett **106**, 163505 (2015).

[8]P. T. H. Fisk, M. J. Sellars, M. A. Lawn and C. Coles, IEEE Trans. Ultrason. Ferroelectr. Freq. Control **44**, 344-354 (1997).

[9]E. A. Burt, W. A. Diener and R. L. Tjoelker, IEEE Trans. Ultrason. Ferroelectr. Freq. Control **55**, 2586-2595 (2008).

[10]J. D. Prestage and G. L. Weaver, Proceedings of the IEEE **95**, 2235-2247 (2007).

[11]P. D. D. Schwindt*, et al.*, *Miniature trapped-ion frequency standard with* $^{171}Yb^{+}$, *Proceedings of the Joint Conference of the IEEE International Frequency Control Symposium & the European Frequency and Time Forum*, Denver, CO, USA, 12-16 April 2015, pp. 752-757.

[12]Y. Y. Jau*, et al.*, Appl Phys Lett **101**, 253518 (2012).

[13]H. Partner, Dissertation, University of New Mexico, 2012.

[14]W. Paul, Reviews of Modern Physics **62**, 531-540 (1990).

[15]P. Fisk, Reports on Progress in Physics **60**, 761 (1997).

[16]J. D. Prestage, R. L. Tjoelker and L. Maleki, *Mercury-ion clock based on linear multi-pole ion trap*, *Proceedings of the IEEE International Frequency Control Symposium*, Kansas City, MO, USA, 7-9 June 2000, pp. 706-710.

[17]R. P. Manginell*, et al.*, Opt Express **20**, 24650-24663 (2012).

[18]S. Jahangir*, et al.*, Journal of Applied Physics **116**, 163511 (2014).

[19]Y.-Y. Jau, J. D. Hunker and P. D. D. Schwindt, AIP Advances **5**, 117209 (2015).

[20]C. Monroe and J. Kim, Science **339**, 1164-1169 (2013).